IDENTIFYING GENES INVOLVED IN [*BIG*$^{+}$] PRION PHENOTYPE

by

JULIA WOOLF

A THESIS

Presented to the Department of Biochemistry
and the Robert D. Clark Honors College
in partial fulfillment of the requirements for the degree of
Bachelor of Science

May 2025

An Abstract of the Thesis of

Julia Woolf for the degree of Bachelor of Science
in the Department of Biochemistry to be taken May 2025

Title: Identifying Genes Involved in [*BIG*$^{+}$] Prion Paromomycin Phenotype

Approved: *David Garcia, PhD*
Primary Thesis Advisor

Prions are self-templating, alternative protein conformations that are inherited through protein-based mechanisms. In *Saccharomyces cerevisiae*, the [*BIG*$^{+}$] prion represents an alternative folding state for the pseudouridine synthase Pus4. When Pus4 undergoes a change in conformation to become [*BIG*$^{+}$], its canonical function modifying uridine-55 in tRNA is maintained. However, the [*BIG*$^{+}$] prion state enhances cellular growth and reduces lifespan under nutrient-rich conditions, likely through increased translation (Garcia et al., 2020; Becker et al., 2017). The molecular mechanisms driving this change remain poorly understood. Notably, [*BIG*$^{+}$] strains exhibit increased sensitivity to paromomycin, an aminoglycoside that induces translational errors, providing a useful qualification of prion presence. Yet, the genetic factors modulating the interaction between [*BIG*$^{+}$] and paromomycin sensitivity remain unknown. This project aims to develop a systematic method for identifying gene deletions impacting [*BIG*$^{+}$] paromomycin sensitivity to determine molecular differences between the prion and naïve cellular states. Using synthetic genetic array (SGA) methodology, prion-containing and naïve query strains were crossed to a NatMX yeast deletion library, and desired haploids were isolated. The growth of these strains was quantitatively assessed under paromomycin stress, and differential growth between prion and naïve backgrounds for each gene deletion strain was analyzed. This approach provides a way to identify genetic pathways influencing [*BIG*$^{+}$] prion propagation, stability, or its effects on translation under paromomycin stress.

Acknowledgements

Thank you to Professor David Garcia, Professor Ellen Fitzpatrick, and Abigail Vaaler-Loftus for serving on my thesis committee. I would also like to thank everyone in my research lab who has helped me learn while I have been a student, either as a peer or a mentor; Sara, Emily, Julia, Preeti, Ethan, Maggie, Will, and especially my mentors Abby and David who have invested a lot of time and energy into helping me grow as a scientist. Thank you, Abby, for always answering any question I have and for being patient as I learn new methods. I have loved being a part of this lab and researching a part of biology that I think is so cool, prions. Being a part of this lab and doing research has been one of my favorite parts of college. To Abby and David, thank you for allowing me the space to explore, make decisions, and fail, while also holding me to a high standard and providing me feedback. I'd also like to thank my brother, Jack Woolf, for always having a spare IMB key and card access, and for letting me use his computer when I couldn't get R to work on mine. Thank you to my roommates for making me coffee as I frantically taught myself, and agonized over, code and statistics in the process of writing this thesis, and for always being my cheerleaders. Thank you to my parents, sister, Kora, grandma, and the Haspelas for offering me endless support and a lot of laughter.

Table of Contents

List of Figures

List of Tables

Introduction

Prions are self-templating proteins that propagate by converting proteins with the same amino acid sequence into an alternative folding pattern. Once formed, prions can aggregate into amyloid-like structures or they can form other assemblies that are fragmented by molecular chaperones, such as heat shock proteins, allowing for continued propagation (Figure 1).

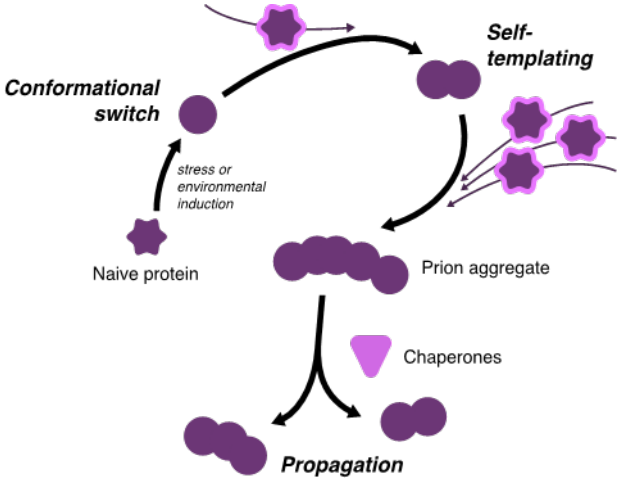

Figure 1. Schematic model of prion induction and propagation.

This conformational shift often results in altered protein function, enabling prions to confer heritable phenotypes without changes to the DNA sequence. While prions are best known for their role in neurodegenerative diseases like Mad Cow Disease, Scrapie, and Chronic Wasting Disease, their discovery in yeast revealed that prions can also provide adaptive advantages (Wickner, 1994). Beneficial yeast prions have been shown to enable cells to metabolize alternative carbon sources (Brown & Lindquist, 2009), resist toxic compounds (Suzuki et al., 2012), and increase size and growth rate (Garcia et al., 2021).

One such prion that can be beneficial in certain environments is [*BIG*$^{+}$] (Garcia et al., 2021). [*BIG*$^{+}$] arises from a conformational change in the RNA-modifying enzyme Pus4. Normally, Pus4 catalyzes the isomerization of uridine to pseudouridine at position U55 on

tRNAs, stabilizing tRNA-ribosome interactions, and modifying select mRNAs (Rintala-Dempsey & Kothe, 2017). In its prion form, Pus4 retains this activity but additionally provides novel phenotypes such as increased cell size, accelerated growth, and enhanced translation, particularly in nutrient-rich environments (Garcia et al., 2021).

Despite these observations, the molecular basis for the [*BIG*$^{+}$] induced phenotypes remains unclear. This project seeks to establish a method for identifying genes and pathways that may interact with [*BIG*$^{+}$] through the examination of a prion-associated phenotype, resistance to paromomycin (Figure 2). Paromomycin is an aminoglycoside antibiotic known to perturb translation.

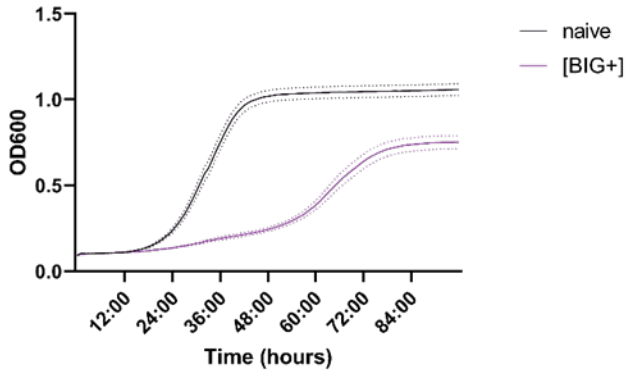

Figure 2. Growth curves of naïve and [BIG+] prion yeast strains in paromomycin containing media.

Naïve (black) and [BIG+] (purple) strains were grown in paromomycin at a concentration of 40 mg/mL. Optical density at 600 nm (OD600) was measured over time to monitor cell growth.

A powerful method for elucidating genetic interactions in yeast is Synthetic Genetic Array (SGA) analysis, which systematically combines a mutation or trait of interest with a genome-wide yeast deletion library to assess the impact of each gene on a given phenotype (Tong & Boone, 2006). In this study, both [*BIG*$^{+}$] and naïve yeast strains were mated to a portion of the yeast deletion library (96 different strains), and the resulting diploids were sporulated.

Haploids were selected for using genetic markers (Figure 4). These strains were then screened on media containing paromomycin to assess differential sensitivity.

In total, the yeast deletion library comprises approximately 6,000 strains, each lacking a single non-essential gene. By comparing growth between [*BIG*$^{+}$] and naïve deletion strains, genes that either suppress or enhance paromomycin sensitivity specifically in the [*BIG*$^{+}$] background can be identified. Such genes are candidates for roles in [*BIG*$^{+}$] propagation, stress response, or translational control.

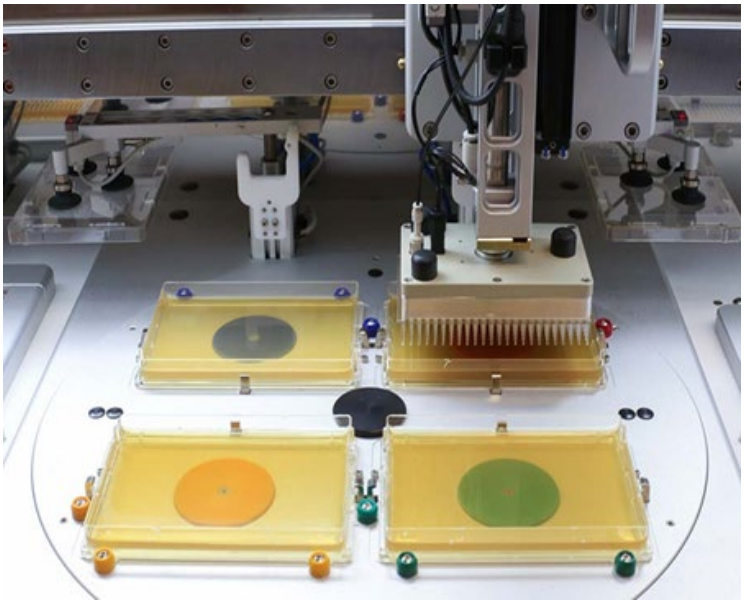

Figure 3. Singer ROTOR.

Robotic pinning of yeast strains onto solid agar media using a Singer ROTOR robot. The 96- or 384-pin head (top right) transfers yeast cultures from source plates onto target plates. Automated pinning ensures consistent inoculum size and spatial uniformity across plates for quantitative growth analysis.

Strains in the pilot screen presented throughout this paper were pinned using hand replica pinners. However, to facilitate high-throughput processing, the screen was planned so that when

scaled up, the Singer ROTOR robot can be used to pin on selective and paromomycin-containing media. This platform enables precise and efficient replication of large strain arrays with flexibility between plate formats and data arrangement, which will be ideal when trying to minimize confounding growth variables and work in different formats.

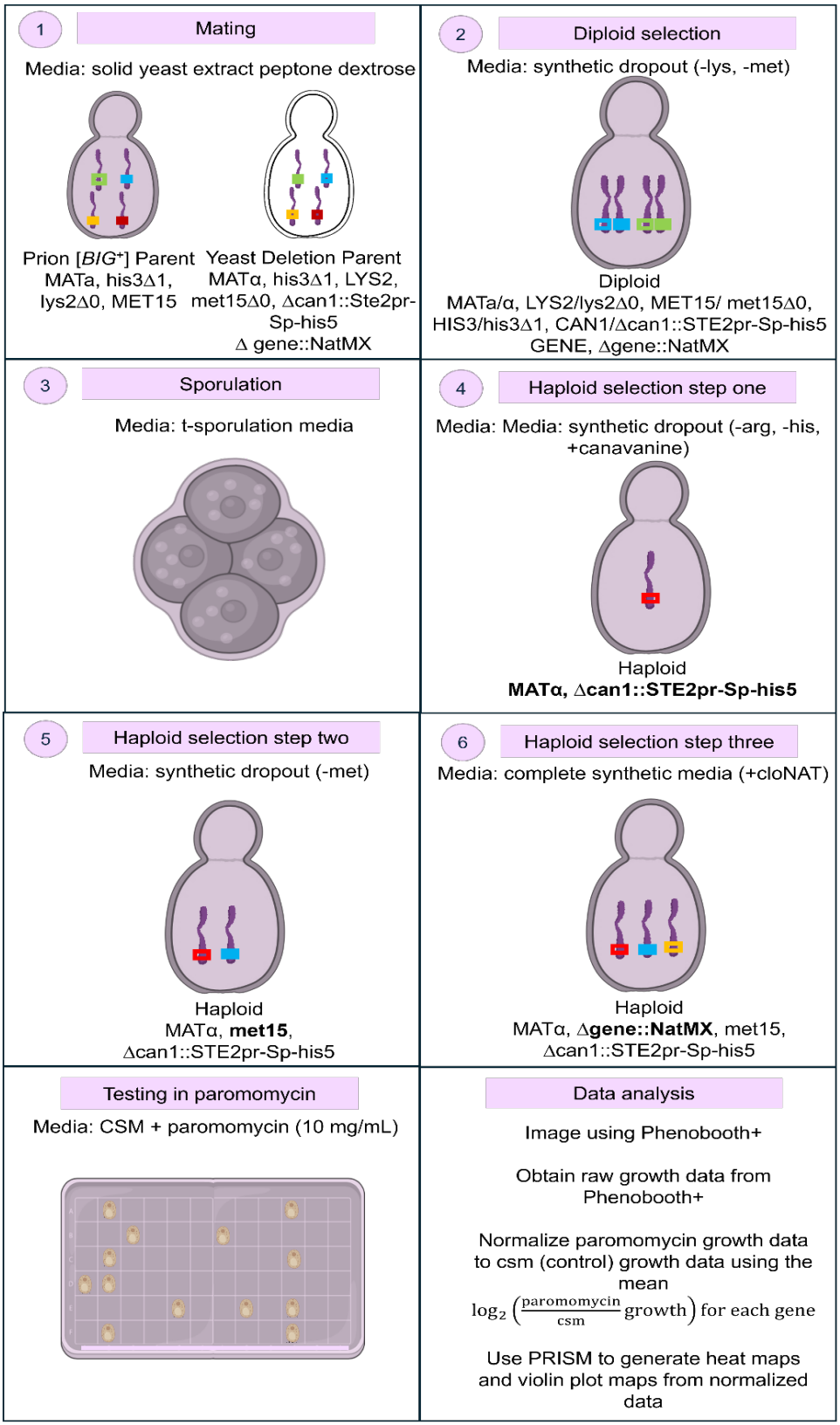

Figure 4. Schematic of Synthetic Genetic Array.

Each panel depicts a different step in the synthetic genetic array. All selection steps and paromomycin sensitivity assays are performed on solid agar media. After the sporulation step, haploid strains were selected in three rounds. The compounding genetic selections are listed below each selection step.

By creating a scalable method to identify gene deletions that modify the [*BIG*$^{+}$] paromomycin phenotype, this work lays the foundation for future, genome-wide screening of molecular interactions with the prion. Additionally, the data generated from differential growth between genes with different backgrounds (prion vs naïve) may broaden our understanding of how prions function beyond pathogenesis, highlighting the genetic basis for their role in adaptive cellular behavior and evolution.

Literature Review

Understanding the development and heritability of complex traits, diseases, and behaviors is important. Inquiries about inheritance and human life have spanned discipline and time, and been topics of religious, philosophical, and scientific debate for thousands of years. Ancient civilizations, such as Mesopotamia, recorded creation myths as early as 4000 BCE (Dalley, 2000), reflecting humanity's long-standing curiosity about the origins and transmission of life. Later, Greek philosophers like Hippocrates, Aristotle, and Plato introduced hypotheses based on naturalistic observations. For example, Aristotle hypothesized that heritable material from both parents combined to form offspring, laying a conceptual foundation for future scientific exploration (Aristotle, 1991).

In the 19th century, Charles Darwin and Gregor Mendel revolutionized our understanding of inheritance, building upon the foundations laid by Greek philosophers. Darwin's observations of finches led him to propose natural selection (Darwin, 1859), while Mendel's pea plant experiments established the basic laws of heredity, that dominant and recessive alleles are passed from parent to offspring (Mendel, 1866). Mendel's and Darwin's data provided evidence for the Mendelian model of genetics, which remains integral to biology and genetics. Unfortunately, Mendelian inheritance alone cannot explain many complex traits such as height, taste preference, or mental health conditions like schizophrenia. Twin studies have shown that these complex traits can vary among individuals with identical genomes, indicating that other, non-genetic mechanisms must also be at play (Bell & Spector, 2011).

These mechanisms are known to be epigenetic, which means they are heritable changes in gene expression that do not alter the DNA sequence. Epigenetic regulation includes DNA methylation, histone modification, RNA-mediated silencing, and chromatin remodeling (Allis &

Jenuwein, 2016). For example, Histone modifications can either expose or shield genes from transcriptional machinery. Open chromatin allows gene expression, while closed chromatin prevents it. This dynamic regulation enables cells to adapt gene expression in response to environmental cues, without any editing of the genome.

One epigenetic mechanism affecting protein function is prion propagation. Prions are proteins that can adopt alternative, self-templating conformations. Prions can recruit and propagate their conformation to other proteins of the same sequence, providing a rapid mechanistic change in response to an environmental cue (Shorter & Lindquist, 2005).

Prions are best known for causing neurodegenerative diseases, including Bovine Spongiform Encephalopathy (Mad Cow Disease), Scrapie in sheep, and Chronic Wasting Disease in cervids (Zabel & Reid, 2015). The first identified human prion disease, Creutzfeldt-Jakob disease, was described by Hans Gerhard Creutzfeldt and Alfons Maria Jakob in the early 20th century (National Institute of Neurodegenerative Disease, 2023) and is characterized by rapid neurodegeneration and death. For many years, the molecular nature of these infectious agents remained unclear, as they did not conform to traditional models of nucleic acid–based inheritance or pathogenicity.

Then, in 1982, Stanley Prusiner demonstrated that the infectious agent responsible for Scrapie was a misfolded protein (Prusiner, 1982), and he called the infectious agent a "prion." Follow-up research confirmed that the same gene encodes both the normal cellular prion protein (PrP^{C}) and the disease-associated form (PrP^{Sc}), differing only in conformation (Moore et al., 1998; Castle & Gill, 2017). PrP prions were shown to aggregate into amyloids and to transmit disease by inducing further misfolding in healthy proteins (Figure 1). Treating cells with guanidine hydrochloride, an Hsp104 inhibitor, can "cure" these prions, further supporting the

idea that these molecules are proteins (Jung & Masison, 2001), whereas the prions are not 'cured' using methods that would denature DNA or RNA such as exposure to UV radiation and treatment with nucleases (Prusiner, 1998).

Yet not all prions are pathogenic. In yeast, prions can serve to provide a functional change for proteins in stressful conditions. Reed Wickner's discovery of the yeast [URE3] prion in 1994 demonstrated that prion-based inheritance could be beneficial (Wickner, 1994). He showed that the Ure2p protein, when converted to the [URE3] form, enabled yeast to utilize poor nitrogen sources. Shortly after, another yeast prion, [*PSI*$^{+}$], was confirmed. [*PSI*$^{+}$] impacted translation termination by modifying the activity of Sup35, resulting in readthrough of stop codons (Cox, 1965; Glover et al., 1997). These phenotypes are inherited through the cytoplasm in a non-mendelian fashion (Figure 5).

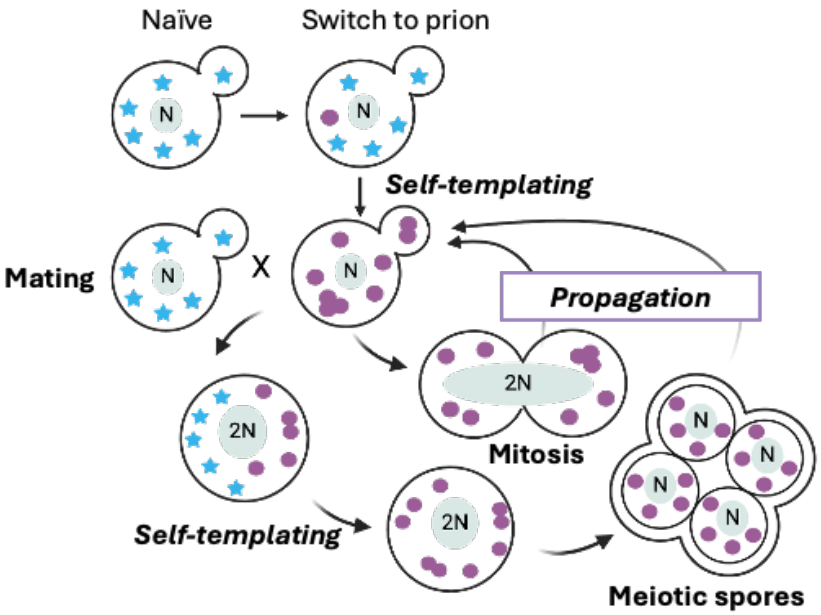

Figure 5. Inheritance patterns for prion proteins and corresponding phenotypes during different division methods.

The prion is inherited through the cytoplasm. During mitosis, both daughter and mother cells are expected to maintain the prion and corresponding phenotype. During meiosis, all daughter cells are expected to inherit the prion and corresponding phenotype.

Today, nearly twenty beneficial yeast prions have been identified (Zhouravleva et al., 2023). Their ability to reversibly respond to stress allows cells to quickly adapt to changing environments, representing a unique form of protein-based epigenetics. One of these prions, [*BIG*$^{+}$], was discovered in 2021 (Garcia et al., 2021). [*BIG*$^{+}$] results from a conformational change in a pseudouridine synthase, Pus4. In its naïve form, Pus4 catalyzes the isomerization of uridine to pseudouridine at position 55 in tRNA (Rintala-Dempsey & Kothe, 2017; Lorenz et al., 2017). In the prion state, the enzyme retains its original function but causes additional phenotypes. These include a larger cell size, faster proliferation, and enhanced translation under rich media conditions (Garcia et al., 2021).

Methods

Parent strain cultivation and growth

All strains were incubated at 30°C unless otherwise noted. Naïve and prion parent strains used in this study are *Sacchromyces cerevisiae* from the BY strain background. All strains were stored at -80°C in 25% glycerol YPD.

Table 1: Starting strains before genetic manipulation

Strain	Phenotype	Genotype	Source
YDG2	Wild-type	BY4742, MATα his3Δ1 leu2Δ0 lys2Δ0 ura3Δ0	Garcia Lab
YDG8	[*BIG*$^{+}$]	BY4742, MATα his3Δ1 leu2Δ0 lys2Δ0 ura3Δ0	Garcia Lab
Boone Deletion Library	Nourseothricin resistant	BY4741, Mat α his3Δ1 leu2Δ0 met15Δ0 ura3Δ0 can1Δ::STE2pr-Sp_his5 lyp1Δ gene Δ::natMX	Boone Lab

Mating Type Switch

CRISPR/Cas9 was used to generate double stranded breaks at the MATα locus of YDG 2 and 8, mimicking HO endonuclease activity (Xie et al., 2018). Plasmid PDG406 was prepped

and transformed into YDG 8 and YDG 2. Transformed colonies were selected on -URA media, and then colonies were streaked on 5-FOA to drop the plasmid out. Mating-type changes were confirmed using a creeping yeast phenotype (Aris et al., 2022).

Strain	Phenotype	Genotype	Source
YDG 2.3	Wild-type	BY4742, MATa his3Δ1 leu2Δ0 lys2Δ0 ura3Δ0	Garcia Lab
YDG 8.1	[BIG^{+}]	BY4742, MATa his3Δ1 leu2Δ0 lys2Δ0 ura3Δ0	Garcia Lab

Table 2: Strains after mating type switch from MATα to MATa

Synthetic genetic array analysis

A [*BIG*$^{+}$] prion strain and a control naïve strain were independently crossed with the Boone yeast deletion library to generate strains for screening. Mating was performed on YPD agar plates. Diploid cells were selected using auxotrophic markers on synthetic dropout media lacking lysine and methionine. Following successful diploid selection, strains were transferred to t-sporulation agar and incubated at 25 °C for five days to induce sporulation.

Haploid selection was carried out through a series of plating steps. First, spores were plated on solid media containing canavanine and lacking arginine (+canavanine / –arginine / -histidine), selecting against diploids and non-sporulated cells. Canavanine is a toxic analog of arginine. Can1 is an arginine importer, meaning that cells without Can1 will not be able to import canavanine and thus will survive. Additionally, because the Can1 locus is replaced with STE2pr-Sp_his5, a his gene with a MATα mating type specific promoter, only MATα strains

will grow on media with canavanine and without histidine. This prevents random mating type assignment from occurring after sporulation, resulting in unwanted diploid formation from mating haploids.

Surviving colonies were then transferred to synthetic dropout media lacking methionine (–methionine) to ensure haploids were being selected where the prion parent strain had been recombined with the yeast deletion library. Then, surviving colonies were selected on yeast peptone dextrose (YPD) media supplemented with clonNAT (+cloNAT), ensuring the yeast deletion was present in each of the strains. At each haploid selection step, drug resistance or auxotrophic selection ensured the isolation of haploid progeny carrying both the gene deletion of interest and either the prion or naïve background.

Unless otherwise specified, plates were incubated for 48 hours at 30 °C between each selection step. Only those haploids that successfully passed through all selection stages were used for subsequent paromomycin sensitivity assays (Figure 4).

Paromomycin sensitivity assays

Strains were cultured for two days on solid YPD agar (when establishing the paromomycin growth phenotype) or harvested from the final stage of haploid selection (during synthetic genetic array). Subsequently, cells were inoculated into 96-well edge plates containing 200 µL of complete supplement media (CSM) per well and incubated at 30 °C for 48 hours. Following incubation, cultures were gently mixed to ensure uniform resuspension. A 5 µL aliquot from each well was transferred to a new 96-well plate containing 200 µL of nanopure water to dilute. Cultures were then immediately pinned from here onto selective plates containing CSM supplemented with 10 mg/mL paromomycin, as well as onto control plates containing CSM without the drug.

High-throughput plating

Mating and plating for query strain growth data crossed to the yeast deletion library was performed manually, using a “hopper” tool. For all other data, a Singer ROTOR robot was used (Figure 3), to pin from a liquid 96-well format to a solid agar 384-well format.

Recording growth data

All solid growth assay data imaging was performed on Phenobooth+ (Figure 6).

Figure 6. Phenobooth+

The Phenobooth is a machine that captures an image of colony growth on solid agar media and converts the image to colony growth data using pixel size.

Processing images

Image processing and analysis was performed using Phenobooth+ and R.

Normalization of colony growth

Growth of prion and naïve strains in paromomycin were normalized using mean $\log_2$ normalization to corresponding strains growing in CSM for each gene (mean $\log_2$(paromomycin/csm)) A small pseudocount value was added for strains so that no growth was divided by zero. This process was performed on R.

Production of heat maps

Heat maps were generated using Graphpad Prism.

Results

Prion strains are sensitive to paromomycin on solid agar media

One member of the Garcia Lab, research assistant Abigail Vaaler Loftus, observed that [*BIG*$^{+}$] cells exhibit increased sensitivity to the paromomycin (Figure 2). Paromomycin is an aminoglycoside antibiotic that targets the ribosomal RNA (rRNA) decoding center of the ribosome, a critical site for ensuring the accurate pairing between mRNA codons and tRNA anticodons during translation. Under normal conditions, the decoding center undergoes conformational changes that verify correct codon–anticodon interactions before allowing peptide bond formation. Paromomycin physically interacts with this region of the ribosome and locks the decoding center into a 'flipped out' conformation, mimicking the state that typically signals a correct match. This artificial stabilization increases the likelihood of incorrect tRNAs being accommodated at the A-site, thereby promoting A-site miscoding and subsequent amino acid misincorporation during translation. As a result, paromomycin treatment can lead to mistranslation, which can impact protein folding, function, and cellular homeostasis; factors particularly relevant when studying how the [*BIG*$^{+}$] prion modulates translation and stress responses (Prokhorova et al., 2017). Somehow, prion strains are being differentially affected by paromomycin's mechanism of action when compared to the naïve strain.

This differential sensitivity provides a useful stress condition that can be used to visualize interactions with genes through use of a yeast deletion library and SGA. In this project, [*BIG*$^{+}$] and naïve strains were crossed to the deletion library, sporulated, and then haploids were selected carrying genetic markers corresponding to elements from the prion parent strain and deletion library parent strain. These markers ensured that the desired haploid would be tested in

paromomycin. The resulting strains were grown on media with or without paromomycin, and their growth was compared.

First, I had to confirm that the prion paromomycin growth phenotype could be observed in a solid media format, as the screen was performed on solid agar media to reduce contamination, observe morphology, and ensure reproducibility. To assess the effect of paromomycin on growth in a solid media format, [*BIG*$^{+}$] prion and naïve yeast strains were pinned onto complete supplement media (CSM) plates with or without 10 mg/mL paromomycin and incubated for two days at 30 °C. Colony size was used as a proxy for relative growth and quantified for statistical comparison.

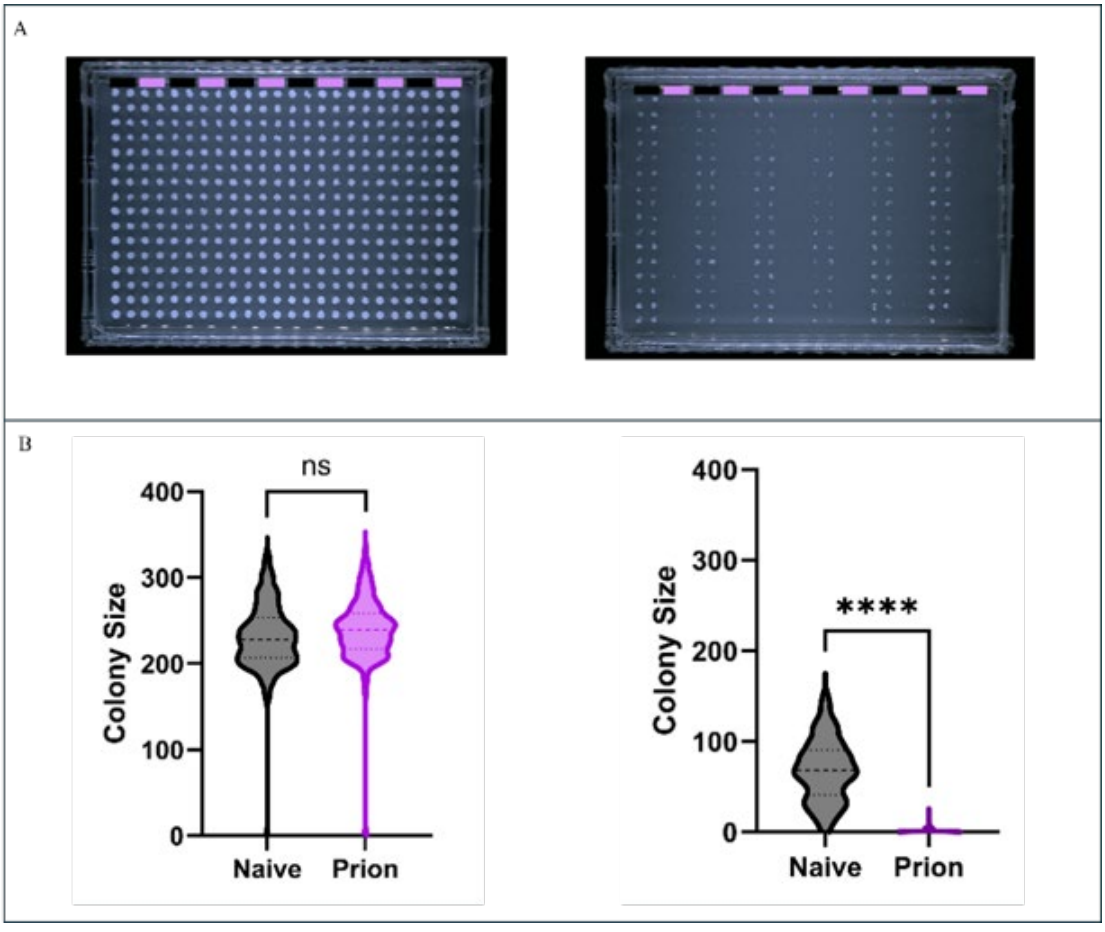

Figure 7. Growth comparisons between prion and naive yeast strains in paromomycin and CSM.

A. Growth of prion and naïve strains YDG 8 and 2 on complete supplement media (left) and complete supplement media with 10mg/mL paromomycin (right). Purple represents a column corresponding to prion growth, while black represents a column of naïve growth data. B. A violin plot of prion and naïve yeast colony size on complete supplement media (left) and paromomycion (right).

As shown in Figure 7, prion and naïve strains displayed comparable growth on control CSM plates lacking drug (Figure 7A and B). Quantification of colony size revealed no significant difference between the two strains under no-stress conditions (violin plot, lower left; unpaired t-test, *ns*, $p > 0.05$), indicating that the [*BIG*$^{+}$] prion does not inhibit growth on nutrient rich media.

However, when cells were grown on CSM with 10 mg/mL paromomycin, (Figure 7A and B) prion strains were more sensitive than naïve control strains. Colonies were visibly smaller, and most of the prion colony growth data was nearly zero. An unpaired t-test confirmed this visual assessment, with a significant reduction in median colony size in prion strains compared to naïve strains (violin plot, lower right; ****, $p < 0.0001$).

These results show that the [*BIG*$^{+}$] prion confers sensitivity to paromomycin on solid agar media, supporting previous findings in the Garcia Lab that the prion strain is sensitive to paromomycin in liquid CSM supplemented with 40 mg/mL of paromomycin (Figure 2). The specific sensitivity to paromomycin suggests that [*BIG*$^{+}$] cells may be more vulnerable to translational perturbation and may be interacting with a translation-related mechanism in yeast cells.

Genetic Screen Confirms Prion-Specific Growth Sensitivity in Paromomycin-Containing Media

To identify genetic modifiers of the prion-induced phenotype in the presence of paromomycin, a high-throughput yeast genetic screen was conducted. This included mating the [*BIG*$^{+}$] and naïve query strains to a yeast deletion library, selecting for diploids, inducing sporulation, and isolating haploids containing single gene deletions in either a prion or naïve background. These strains were subsequently grown on solid media supplemented with 10 mg/mL paromomycin, and colony size was evaluated.

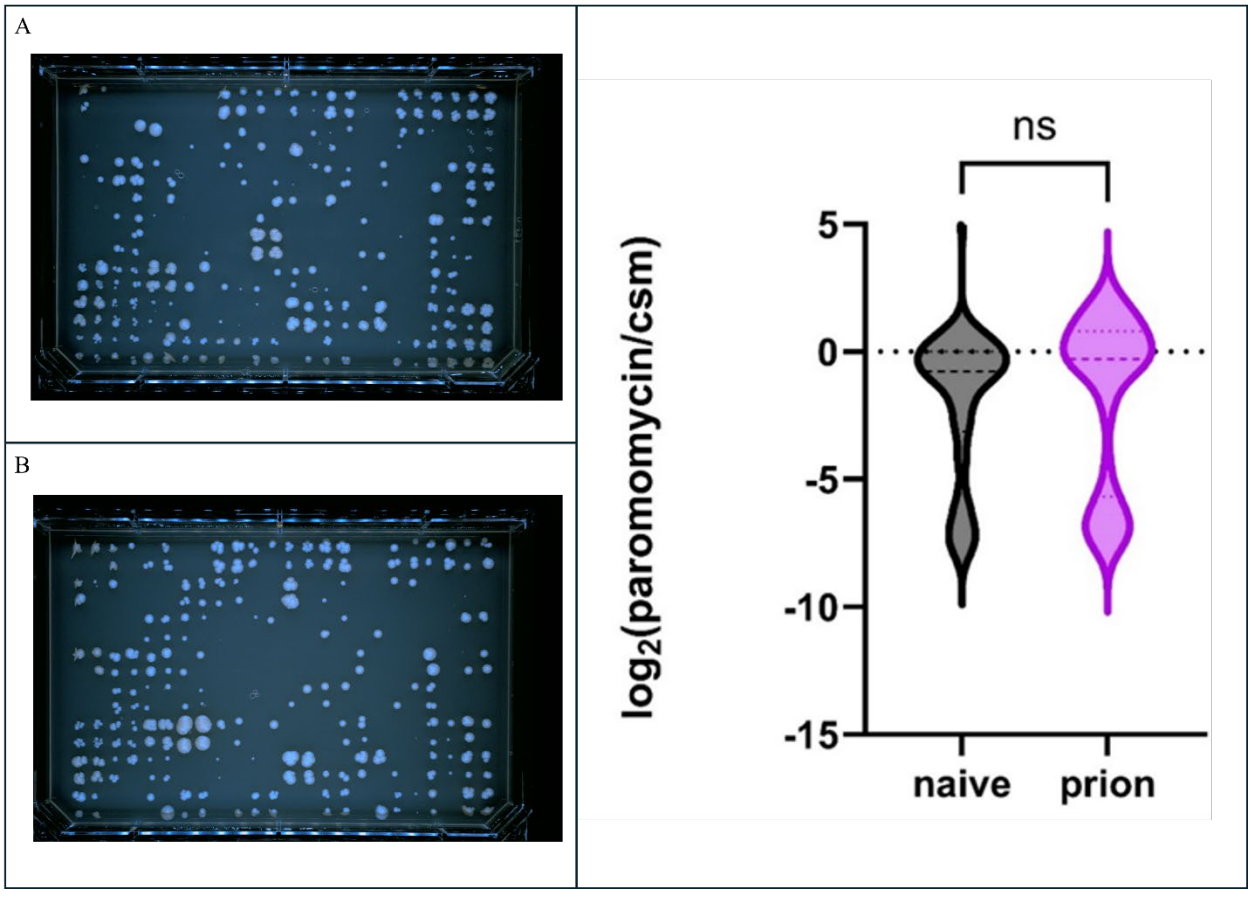

Figure 8. Global growth comparison in paromomycin between haploid naïve and prion yeast deletion strains that have undergone selection (Figure 4).

A. Naïve yeast deletion library strain in paromomycin B. Prion yeast deletion library strain in paromomycin. C. The mean of each group of four gene deletion replicates was taken for both the naïve and prion strains. Growth on paromomycin for the gene deletion was then normalized to growth for the corresponding gene deletion on CSM using $\log_2$ normalization.

Growth data was normalized as $\log_2$(paromomycin/CSM growth) colony sizes, so that comparisons could be made between the prion and naïve data. Violin plot distributions of all gene deletion strains summed together (Figure 8) revealed a broad range of paromomycin sensitivity across both backgrounds. Additionally, there was generally a skew downward in the violin plot for both the naïve and prion yeast deletion strains in comparison to the previous naïve and prion strains without gene deletions (Figure 7), indicating poorer growth in paromomycin overall when the gene deletions are introduced. However, the mean $\log_2$-transformed growth values were not significantly different between the naïve and prion-containing populations (*ns*, $p > 0.05$). This suggests that while many gene deletions strongly affect prion-specific sensitivity to paromomycin, some of these effects may be heterogeneous. These data points emphasize the need to analyze specific gene-level differences, rather than relying on global summary statistics, to uncover the genetic dependencies of the [*BIG*$^+$] prion under translational stress.

Next, a gene-level analysis was performed. Growth data for each gene deletion strain that had undergone selection (Figure 4) was analyzed using $\log_2$ normalization, comparing growth in paromomycin to growth in CSM. In this analysis, a normalized score of 0 indicates no growth difference between paromomycin and CSM conditions for that strain. A positive score indicates that the strain grew better in paromomycin than in CSM, while a negative score indicates better growth in CSM than in paromomycin. To assess the differential effect of the [BIG$^+$] prion, normalized growth scores for the prion strain were compared to the corresponding naïve strain by calculating the difference: prion $\log_2$(normalized growth) − naïve $\log_2$(normalized growth) (Table 3). In this comparison, negative values indicate gene deletions where the naïve strain

outgrew the prion strain in paromomycin, whereas positive values indicate gene deletions where the prion strain outgrew the naïve strain.

Table 3. Normalized growth data and differences in prion and naïve normalized data

Gene	naive mean log2 normalized growth data	prion mean log2 normalized growth data	change in growth (prion - naïve)
ALF1	0.609944857	-5.693486957	-6.303431815
AMN1	-1.236067358	-0.383755409	0.852311949
APQ12	-1.942918905	1.209051333	3.151970238
ASE1	0.572949983	-0.212330966	-0.785280949
BIK1	-6.21916852	-0.072979445	6.146189075
BUB1	1.02676691	2.156433892	1.129666982
BUB2	0	0.975826326	0.975826326
BUB3	-7.658211483	-6.710806434	0.947405049
CDC40	0	0.355636206	0.355636206
CDC55	0.344549892	-5.599912842	-5.944462734
CHK1	-1.06871275	-0.10496956	0.96374319
CIN1	-6.731319031	-6.77807713	-0.046758099
CKA1	-0.667424661	-0.685180138	-0.017755477
CKA2	-7.902375114	-7.436711542	0.465663572
CKB1	-4.06486984	-4.075767508	-0.010897668
CKB2	-4.92691765	-4.72597481	0.20094284
DBF2	0.877881918	1.701052718	0.8231708
DBF20	-0.110444821	-0.489965987	-0.379521166
DMA1	0	-5.794415866	-5.794415866
DMA2	-0.202816883	1.295128036	1.497944919
DUN1	-1.005517005	-1.550920927	-0.545403922
DYN3	4.894817763	-6.303780748	-11.19859851
ELM1	0.128535958	0.222979479	0.094443521
GIN4	-0.594240314	-7.355351096	-6.761110782
GRH1	0.059971022	1.849105271	1.78913425
HSL1	-4.121410173	-0.285643978	3.835766196
IBD2	-0.761595261	-0.912407601	-0.15081234
IME2	-2.493408563	-0.63297675	1.860431812
JSN1	-0.788044747	-7.116343961	-6.328299214
KAR9	-0.892723264	-7.278449458	-6.385726195
KCC4	-5.851749041	-5.614709844	0.237039197
KIN82	-0.594229479	-0.331549661	0.262679818
KIP2	-0.086201035	-0.767615807	-0.681414772
KIP3	-0.754056696	0.862496476	1.616553172
MAD1	-0.107432429	0.998301713	1.105734141
MAD2	-0.911385613	0.411964665	1.323350278
MAD3	1.066474278	1.658692889	0.592218611
MDS3	-0.241786672	-6.54303182	-6.301245148

MEK1	-6.988684687	-1.938599455	5.050085231
MUM2	0	-0.313157885	-0.313157885
NAM8	-0.620824	-6.74819285	-6.12736885
NUM1	-6.885696373	-7.011227255	-0.125530882
PAC1	-3.028196892	-0.106389345	2.921807547
PAC11	-1.372477037	-0.141807326	1.230669711
PAC2	-2.75802721	-2.231591358	0.526435852
PFD1	0.789951876	1.299560282	0.509608406
PHO13	-3	-0.700098211	2.299901789
PHO8	-0.539552041	-6.640244936	-6.100692895
PHR1	0.096037337	0.814208593	0.718171257
POL32	-8.171176798	-6.654636029	1.516540769
PPH21	0.32910732	1.272459419	0.943352098
PPH22	0.174174474	1.035166854	0.86099238
PPS1	-1.047866311	-0.37166999	0.676196321
PRK1	-0.35687616	-0.238091108	0.118785052
PSD2	-7.28771238	-7.144658243	0.143054137
RAD14	-2.189172886	0	2.189172886
RAD16	-6.569855608	-7.055282436	-0.485426827
RAD2	0.018804401	-0.362865805	-0.381670206
RAD23	-0.911049077	2.034240324	2.945289402
RAD26	0.730579959	0	-0.730579959
RAD4	-0.705627628	-7.413627929	-6.708000301
RAD7	-2.458414562	0.333972131	2.792386692
RCK1	0.375568125	0.272661577	-0.102906548
RCK2	-1.029029049	0.325811529	1.354840578
REG1	0.372396523	-6.290018847	-6.66241537
RIM15	-0.674250194	1.077305726	1.75155592
RMD5	-7.226412193	-6.348728154	0.877684039
RTS1	-0.424966617	-2.2472177	-1.822251084
RTS3	-7.665335917	1.503766418	9.169102335
RTT103	-1.658963082	-7.759888183	-6.100925101
RTT106	-1.045229254	1.894506871	2.939736125
RTT107	-1.871992388	-0.528928466	1.343063922
RTT109	-7.411510988	-6.717676423	0.693834565
RUB1	-1.492032191	0.563301718	2.055333909
SAK1	-6.693486957	0.031066198	6.724553156
SLI15	0.190986617	2.049457481	1.858470864
SPC72	-1.944958636	-0.172404286	1.772554351
SPO13	-5.924812504	-1.727670702	4.197141801
SRL1	0.921390165	2.252830155	1.331439989
SRL2	-1.478208826	0.553622098	2.031830924
SRL3	-6.527477006	1.179447776	7.706924782
STI1	0.471247892	0.495810123	0.024562231
SYF2	0.057421635	-0.8945837	-0.952005335

TUB3	-7.405141463	0.784271309	8.189412772
UBP15	-0.778710135	-5.839203788	-5.060493653
UBP5	-0.050137306	0.883806982	0.933944288
VHS1	-0.125236184	-0.684102319	-0.558866135
VID28	-5.735904399	-7.636624621	-1.900720222
YAK1	0.605779034	0.158916479	-0.446862556
YCK3	-3.167814255	-7.407267764	-4.239453509
YHP1	-0.654310547	1.26072054	1.915031087
YKE2	-0.645963573	1.084722679	1.730686252
YOX1	-7.573647187	-0.370140961	7.203506226
YPK2	-0.164386818	0.21161795	0.376004768
YTA7	-0.476237656	0.982346135	1.458583791
ZUO1	-3.977279923	-0.185765989	3.791513934

Paromomycin data was normalized to CSM data, and then normalized naïve data was subtracted from normalized prion data to get differential growth.

Data from Table 3 was plotted on a heatmap (Figure 9). Each row represents a deletion strain, and the color intensity reflects the growth difference in paromomycin, mathematically defined as the prion strain's $\log_2$(growth in paromomycin/growth in CSM) – the naïve strain's $\log_2$(growth in paromomycin/ growth in CSM). Orange values near zero indicate similar growth between backgrounds, while yellow positive or dark purple negative values denote enhanced or impaired growth in the prion strain, respectively. Despite the overall mean effect being statistically nonsignificant (Figure 8), the heatmap demonstrates that several deletions result in differential growth data between the prion and naïve strains.

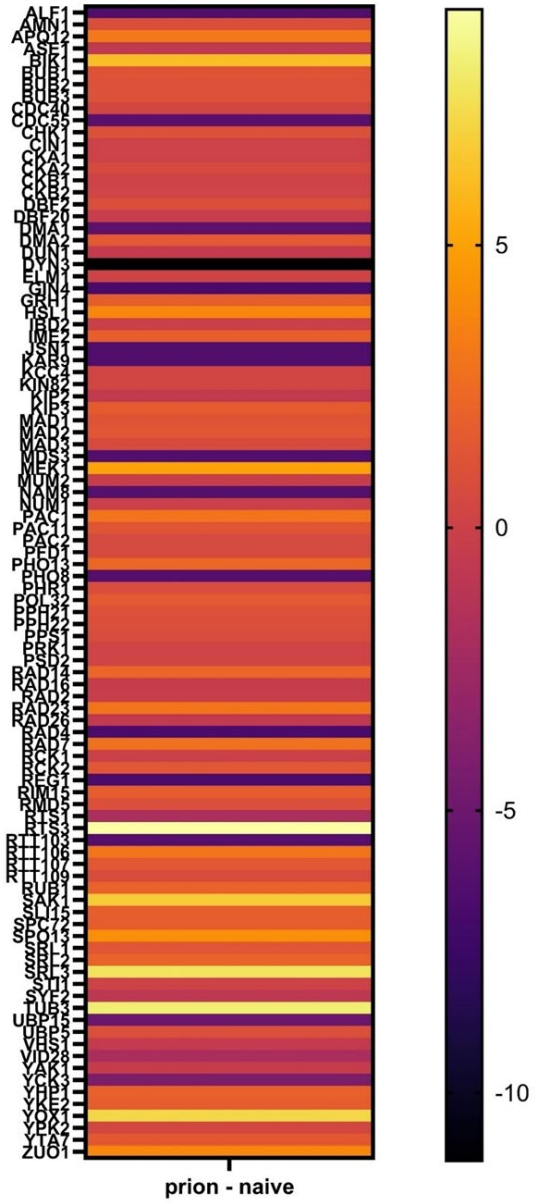

Figure 9. Heatmap depicting grow differences between normalized growth data for prion and naïve yeast deletion library strains.

Deletions of genes such as ZUO1, RAD7, RTT106, and TUB3 show strong negative values, suggesting that their absence exacerbates the [*BIG*$^{+}$] prion growth defect in paromomycin. These genes are involved in translation fidelity, chromatin organization, and cytoskeletal function (Gillette et al., 2006; Yan et al., 1998; Imbeault et al., 2008; Schatz et al.,

1986), which aligns with previously reported [*BIG*$^{+}$] vulnerabilities. Garcia et al. (2021) demonstrated that [*BIG*$^{+}$] strains exhibit heightened sensitivity to translation stress and proteotoxic stress, likely due to their increased translational activity and altered protein homeostasis. For example, ZUO1, a ribosome-associated chaperone that promotes translation fidelity and nascent chain folding, may be important for buffering the high translational stress in [*BIG*$^{+}$] cells. Loss of ZUO1 would therefore be expected to further destabilize protein quality control, leading to exacerbated growth defects under aminoglycoside-induced mistranslation. Similarly, chromatin-related genes such as RAD7 and RTT106 may influence gene expression programs that support cellular adaptation to proteotoxic stress, while TUB3, an α-tubulin isoform, could impact cytoskeletal dynamics important for stress resilience and cell division under prion-induced translational strain.

In contrast, deletions of genes such as HSL1, SAK1, and SPO13 exhibit strong positive values (Figure 9, Table 4), suggesting that loss of these genes partially suppresses the prion growth defect under translational stress. These genes are involved in cell cycle regulation and metabolism (Schulewitz et al., 1999; Orlova et al., 2010; Shonn et al., 2002). One interpretation is that modulation of cell cycle checkpoints can buffer the deleterious effects of prion-induced mistranslation. For example, slowing cell cycle progression may give cells more time to manage misfolded proteins or adjust translation under stress conditions. Another interpretation of this data is that these genes may be involved in the propagation or maintenance of the prion.

The top and bottom ten differential growth values, along with functional annotations drawn from the Saccharomyces Genome Database, are summarized in Table 4. These results reinforce the model that [*BIG*$^{+}$] sensitizes cells to translation-related stresses, consistent with findings from Garcia et al. (2021). In the future, this screening method can be used to identify

new candidate pathways that may modulate prion phenotypes or provide protective mechanisms under conditions of translational stress, but after only a pilot screen there is not enough evidence to conclusively identify any particular mechanisms.

Top ten growth genes	Gene product information from SGD	Bottom ten growth genes	Gene product information from SGD
RTS3	unknown function, localizes to the nucleus and cytoplasm	DYN3	a part of dyenein (a motor protein that moves along microtubules) . Null mutants cannot undergo nuclear migration
TUB3	alpha-tubulin; associates with TB2p to form tubulin dimer	GIN4	a protein kinase involved in bud growth and septin ring assembly (important for cytokenesis)
SRL3	localizese to cytoplasm, binds to RNA polymerase II and suppresses START	RAD4	Damaged-DNA binding subunit of Nuclear Excision Repair Factor 2; recognizes and binds damaged DNA with Rad23p during nucleotide excision repair (NER); also involved with Rad23p in turnover of ubiquitylated proteins; Rad4p-Rad23p heterodimer binds to promoters of DNA damage response genes to repress their transcription in the absence of DNA damage; RAD4 and RAD51 pathways confer resistance to benzo[a]pyrene dihydrodiol
YOX1	transcriptional repressor binding to Mcm1p and to ECBs in the promoters of cell cycle-regulated genes. Phosphorylated by Cdc28p. When DNA replication stress occurs, Cdc28p relocalizes from nucleus to cytoplasm	REG1	Regulatory subunit of type 1 protein phosphatase Glc7p; involved in negative regulation of glucose-repressible genes; involved in regulation of the nucleocytoplasmic shuttling of Hxk2p; REG1 has a paralog, REG2, that arose from the whole genome duplication
SAK1	serine/threonine kinase for SNF1 complex. Regulation of energy metabolism in response to stress or nutrient deprivation	KAR9	Spindle positioning factor; orients astral microtubules, connecting them to actin cables at the cortex with Bim1p and Myo2, resulting in proper spindle positioning; targeted for StuBL-dependent degradation at kinetochores by Slx5p-Slx8p, ensuring chromosome transmission fidelity and correct spindle positioning; role in karyogamy; localizes to the shmoo tip, the growing bud-tip, the nucleus, the kinetochore, the spindle and microtubules; homolog of adenomatous polyposis coli
BIK1	Microtubule-associated protein that stabilizes kip2p plus ends and recruits kip2p to mitotic SPBs	JSN1	Member of the Puf family of RNA-binding proteins; interacts with mRNAs encoding membrane-associated proteins; involved in localizing the Arp2/3 complex to mitochondria; overexpression causes increased sensitivity to benomyl; JSN1 has a paralog, PUF2, that arose from the whole genome duplication
MEK1	meiosis-specific serine/threonine protein kinase functioning in meiotic checkpoint	ALF1	Alpha-tubulin folding protein; similar to mammalian cofactor B; Alf1p-GFP localizes to cytoplasmic microtubules; required for the folding of alpha-tubulin and may play an additional role in microtubule maintenance
SPO13	meiotic regulator that is involved in maintaining sister chromatid cohesion, promotes attachment of kinetochores to the spindle during meiosis I and II	MDS3	Putative component of the TOR regulatory pathway; negative regulator of early meiotic gene expression; required, with Pmd1p, for growth under alkaline conditions; has an N-terminal kelch-like domain; MDS3 has a paralog, PMD1, that arose from the whole genome duplication
HSL1	protein kinase related to NIM1p, a protein that controls progression from G1 phase to S phase	NAM8	RNA binding protein, component of the U1 snRNP protein; mutants are defective in meiotic recombination and in formation of viable spores, involved in the formation of DSBs through meiosis-specific splicing of REC107 pre-mRNA; Nam8p regulon embraces the meiotic pre-mRNAs of REC107, HFM1, AMA1 SPO22 and PCH2; the putative RNA binding domains RRM2 and RRM3 are required for Nam8p meiotic function
ZUO1	ribosome-associated co-chaperone that acts as a chaperone for polypeptide chains as they are being created, and acts in ribosome biogenesis	RTT103	Protein implicated in transcription termination by RNA polymerase II; binds to the RNA polymerase II C-terminal domain (CTD) phosphorylated on serine (ser2); interacts with 5' to 3' exonuclease Rat1p and decapping endonuclease Rai1p and is involved in mRNA 3' end processing; contains an RPR domain (CTD-interacting domain); involved in regulation of Ty1 transposition [1] [2] [3]

Table 4. Gene deletions resulting in the largest growth differences between prion and naïve strains.

Gene deletions are plotted with a summary of their function from SGD

Discussion

The [*BIG*$^{+}$] prion presents a model for exploring how protein-based inheritance can influence cellular physiology in response to environmental stress. While previous studies from the Garcia Lab demonstrated that [*BIG*$^{+}$] enhances translation and growth in nutrient-rich environments, this project set out to establish a method for uncovering the molecular underpinnings of its differential phenotypes. The identification of [*BIG*$^{+}$] paromomycin phenotype on solid agar provided a way to evaluate both the presence of the prion and differential growth data, indicating genes potentially interacting with the prion or involved in pathways impacting the prion.

The initial growth assays confirmed that [*BIG*$^{+}$] cells are significantly more sensitive to paromomycin on solid agar media than their naïve counterparts, consistent with prior findings (Figure 7). Importantly, this phenotype is not due to a general growth defect, as prion and naïve strains grow equivalently on control plates lacking drug. Instead, the data support a model in which [*BIG*$^{+}$] cells are selectively vulnerable to translational disturbance. Given that paromomycin interferes with ribosome fidelity and potentially induces miscoding (Eustice et al. 1984), the hypersensitivity of [*BIG*$^{+}$] cells suggests that the prion state may be interacting with translation machinery or regulation differently than the naïve state. Something about the prion strain makes translation more susceptible to perturbation.

The genetic screen of the selected spores from a generated prion and naïve yeast deletion library revealed that this sensitivity is not globally consistent, but gene specific. There was a wide range of outcomes across the deletion library. The violin plot analysis of the full dataset showed no significant shift in mean growth between the prion and naïve populations (Figure 8),

yet heatmap visualization illuminated a heterogeneous set of responses, ranging from rescue to exacerbation of the prion phenotype (Figure 9).

A closer look at the gene-specific data highlights many significant differences between the prion and naïve background for the same gene deletions. Deletions of ZUO1, TUB3, RAD7, and RTT106 significantly increased the paromomycin sensitivity of [*BIG*$^{+}$] strains in comparison to the naïve strains. The products of these genes are involved in ribosome quality control, cytoskeletal structure, DNA repair, and chromatin remodeling, respectively. Their compounding impact on the prion phenotype in paromomycin suggests that they may be involved in a pathway buffering the translational stress imposed by the prion state. Conversely, deletions of HSL1, SAK1, and SPO13, which are involved in cell cycle regulation and stress signaling, masked the prion phenotype in paromomycin, or resulted in an inability of the prion to propagate across generations. In the first case, these data points potentially indicate that some stress pathways or molecular activity may overcompensate and become detrimentally overactive when [*BIG*$^{+}$] cells undergo translational pressure. It is also possible that these pathways are involved in regulating the cell when translation machinery is compromised, in this case due to the potential compounding effect paromomycin and the prion have on the rate and fidelity of translation. It is possible these genes are guarding against an overgrown state for the cell and that some of these genes are involved in slowing cell growth by slowing translation rates and thus avoiding a dysfunctional proteome generated by dysregulated translation, resulting in fast growth when they are deleted.

Alternatively, it is also possible that some cells lost the prion during sporulation, which could account for the loss of paromomycin sensitivity observed in certain gene deletions. Since sporulation occurs under near-starvation conditions, and Garcia et al. have shown that the [*BIG*$^{+}$]

prion is not beneficial during starvation, it may be advantageous for cells to lose the prion under these conditions. To test this possibility, a future experiment should be performed in which a haploid prion is crossed to a naïve strain (without any gene deletion) and is sporulated using the same protocol applied during the prion and yeast deletion library cross (Figure 4). The resulting haploids would then be grown in paromomycin to assess the rate of prion loss after sporulation. Colonies that show a loss of paromomycin sensitivity would indicate cells where the prion was lost during the process, which would then provide information about how many gene deletion strains may lose the prion during the screening process.

Overall, the data support a model in which [*BIG*$^{+}$] creates a sensitized cellular state. The pilot screen successfully demonstrated the feasibility of this approach, as evidenced by the identification of multiple genetic 'hits.' Moving forward, it will be important to refine this method to yield a more focused set of candidate genes. This could be achieved by optimizing the paromomycin concentration used during the drug assay or by exploring additional analytical methods to enhance specificity and sensitivity. Future studies should expand upon this framework to conduct larger-scale genetic analyses that systematically link gene deletions to prion-associated growth phenotypes. In particular, applying this approach to the full yeast deletion library will provide a comprehensive view of the genetic landscape influencing [*BIG*$^{+}$] and the cell. In the near future, I plan to apply this approach to the entire yeast deletion library, with the goal of uncovering new pathways and factors that modulate [*BIG*$^{+}$] propagation and its cellular effects. Other outcomes of this project will include the generation of an entire prion yeast deletion library that can be used in later projects.

Additionally, the naïve yeast deletion library generated could provide interesting and novel information about the genetic interactions between a naïve cell and paromomycin, as a NatMX gene deletion library has not been tested in paromomycin before.

Conclusion

By identifying genetic factors that interact with the [*BIG*$^{+}$] prion under paromomycin induced translational stress, this project provides a foundation for dissecting the molecular mechanisms of prion biology and prion-induced phenotypes. Gene deletions that destabilize or promote loss of [*BIG*$^{+}$] or masking the [*BIG*$^{+}$] phenotype may offer insight into the cellular machinery required for prion propagation, including potential roles for chaperones, protein folding pathways, and quality control systems. Conversely, deletions that alter the sensitivity of [*BIG*$^{+}$] strains to paromomycin, without affecting prion maintenance, can reveal downstream pathways modulated by the prion, such as translation factors, tRNA modification enzymes, or stress response networks. Additionally, identifying gene deletions that influence prion induction may uncover conditions or pathways that trigger [*BIG*$^{+}$] formation. Together, these genetic interactions will help distinguish between core components of prion biology and the broader cellular processes that contribute to prion-driven phenotypes. Ultimately, this approach establishes a valuable framework for systematically mapping the functional network of [*BIG*$^{+}$] and advancing our understanding of how protein-based inheritance can reshape cellular physiology.

Prion biology offers insights reaching beyond yeast and prion diseases. At its core, prion-based inheritance challenges the traditional view that heredity is controlled solely by DNA. Instead, prions show that protein shape alone can carry biological information, and that this information can be stably inherited across generations. In humans, this concept helps explain why disease mechanisms can be hard to identify and can also provide information about a cell's ability to respond rapidly to stress without alteration of the genetic code. In yeast, prions like [*BIG*$^{+}$] reveal how protein-based changes can rewire fundamental processes like translation and

growth, which are processes conserved across life. By uncovering the genetic pathways that interact with prions, this work can help us understand not only how cells manage stress, but also how life encodes flexibility beyond the genome.

Bibliography

Allis, C. D., & Jenuwein, T. (2016). The molecular hallmarks of epigenetic control. *Nature Reviews Genetics*, 17(8), 487–500. https://doi.org/10.1038/nrg.2016.59

Aristotle. (1991). *Generation of animals* (A. L. Peck, Trans.). Harvard University Press. (Original work published ca. 350 B.C.E.)

Becker, H. F., Motorin, Y., Planta, R. J., & Grosjean, H. (1997). The yeast gene YNL292w encodes a pseudouridine synthase (Pus4) catalyzing the formation of psi55 in both mitochondrial and cytoplasmic tRNAs. *Nucleic Acids Research, 25*(22), 4493–4499. https://doi.org/10.1093/nar/25.22.4493

Bell, J. T., & Spector, T. D. (2011). A twin approach to unraveling epigenetics. *Trends in Genetics*, 27(3), 116–125. https://doi.org/10.1016/j.tig.2010.12.005

Brown, J. C. S., & Lindquist, S. (2009). A heritable switch in carbon source utilization driven by an unusual yeast prion. *Genes & Development, 23*(19), 2320–2332. https://doi.org/10.1101/gad.1839109

Castle, A. R., & Gill, A. C. (2017). Physiological functions of the cellular prion protein. *Frontiers in Molecular Biosciences, 4*, 19. https://doi.org/10.3389/fmolb.2017.00019

Cox, B. S. (1965). Ψ, a cytoplasmic suppressor of super-suppressor in yeast. *Heredity, 20*(4), 505–521. https://doi.org/10.1038/hdy.1965.65

Dalley, S. (2000). *Myths from Mesopotamia: Creation, the Flood, Gilgamesh, and Others* (Revised Edition). Oxford University Press.

Darwin, C. (1859). *On the origin of species by means of natural selection, or the preservation of favoured races in the struggle for life*. London: John Murray. Retrieved from https://darwin-online.org.uk/content/frameset?itemID=F373&viewtype=text&pageseq=1

Garcia, D. M., Campbell, E. A., Jakobson, C. M., Tsuchiya, M., Shaw, E. A., DiNardo, A. L., Kaeberlein, M., & Jarosz, D. F. (2021). A prion accelerates proliferation at the expense of lifespan. *eLife, 10*, e60917. https://doi.org/10.7554/eLife.60917

Glover, J. R., Kowal, A. S., Schirmer, E. C., Patino, M. M., Liu, J. J., & Lindquist, S. (1997). Self-seeded fibers formed by Sup35, the protein determinant of [PSI+], a heritable prion-like factor of S. cerevisiae. *Cell, 89*(5), 811–819. https://doi.org/10.1016/S0092-8674(00)80264-0

Jung, G., & Masison, D. C. (2001). Guanidine hydrochloride inhibits Hsp104 activity in vivo: A possible explanation for its effect in curing yeast prions. *Current Microbiology, 43*(1), 7–10. https://doi.org/10.1007/s002840010251

Lorenz, C., Lünse, C. E., & Mörl, M. (2017). tRNA modifications: Impact on structure and thermal adaptation. *Biomolecules, 7*(2), 35. https://doi.org/10.3390/biom7020035

Maher, B. (2008). Personal genomes: The case of the missing heritability. *Nature, 456*(7218), 18–21. https://doi.org/10.1038/456018a

Mendel, G. (1866). *Experiments in plant hybridization*. *Verhandlungen des naturforschenden Vereines in Brünn*, 4, 3–47. (English translation available at https://www.esp.org/foundations/genetics/classical/gm-65.pdf).

Moore, R. C., Hope, J., McBride, P. A., McConnell, I., Selfridge, J., Melton, D. W., & Manson, J. C. (1998). Mice with gene-targeted prion protein alterations show that Prnp, Sinc and Prni are congruent. *Nature Genetics, 18*(2), 118–125. https://doi.org/10.1038/ng0298-118

NINDS. (2023). *Creutzfeldt-Jakob disease*. National Institute of Neurological Disorders and Stroke. https://www.ninds.nih.gov/health-information/disorders/creutzfeldt-jakob-disease

Prokhorova, I., Altman, R. B., Djumagulov, M., Shrestha, J. P., Urzhumtsev, A., Ferguson, A., Chang, C.-W. T., Yusupov, M., Blanchard, S. C., & Yusupova, G. (2017). Aminoglycoside interactions and impacts on the eukaryotic ribosome. *Proceedings of the National Academy of Sciences, 114*(51), E10899–E10908. https://doi.org/10.1073/pnas.1715501114

Prusiner, S. B. (1982). Novel proteinaceous infectious particles cause scrapie. *Science, 216*(4542), 136–144. https://doi.org/10.1126/science.6801762

Prusiner, S. B. (1998). Prions. *Proceedings of the National Academy of Sciences*, 95(23), 13363–13383. https://doi.org/10.1073/pnas.95.23.13363

Prokhorova, I., Altman, R. B., Djumagulov, M., Shrestha, J. P., Urzhumtsev, A., Ferguson, A., Chang, C.-W. T., Yusupov, M., Blanchard, S. C., & Yusupova, G. (2017). Aminoglycoside interactions and impacts on the eukaryotic ribosome. *Proceedings of the National Academy of Sciences of the United States of America*, *114*(52), E10899–E10908. https://doi.org/10.1073/pnas.1715501114

Rintala-Dempsey, A. C., & Kothe, U. (2017). Eukaryotic stand-alone pseudouridine synthases—RNA modifying enzymes and emerging regulators of gene expression? *RNA Biology, 14*(9), 1185–1196. https://doi.org/10.1080/15476286.2016.1276150

Shorter, J., & Lindquist, S. (2005). Prions as adaptive conduits of memory and inheritance. *Nature Reviews Genetics*, 6(6), 435–450. https://doi.org/10.1038/nrg1616

Suzuki, G., Shimazu, N., & Tanaka, M. (2012). A yeast prion, Mod5, promotes acquired drug resistance and cell survival under environmental stress. *Science, 336*(6079), 355–359. https://doi.org/10.1126/science.1219491

Tong, A. H. Y., & Boone, C. (2006). Synthetic genetic array analysis in Saccharomyces cerevisiae. In *Methods in Molecular Biology* (Vol. 313, pp. 171–192). https://doi.org/10.1385/1-59259-958-3:171

Wickner, R. B. (1994). [URE3] as an altered URE2 protein: Evidence for a prion analog in Saccharomyces cerevisiae. *Science, 264*(5158), 566–569. https://doi.org/10.1126/science.7909170

Zabel, M. D., & Reid, C. (2015). A brief history of prions. *Pathogens and Disease, 73*(9), ftv087. https://doi.org/10.1093/femspd/ftv087

Zhouravleva, G. A., Bondarev, S. A., & Trubitsina, N. P. (2023). How big is the yeast prion universe? *International Journal of Molecular Sciences, 24*(14), 11651. https://doi.org/10.3390/ijms241411651